A Novel MILP Scheduling Model for Power-Intensive Processes under Time-Sensitive Electricity Prices

Natalia P. Basán[†], *Ignacio E. Grossmann*[‡], *Ajit Gopalakrishnan*[§], *Irene Lotero*[§], *Carlos A. Méndez*[†*]

[†] INTEC (UNL –CONICET), Güemes 3450, Santa Fe, 3000, Argentina

[‡] Chemical Engineering, Carnegie Mellon University, Pittsburgh, United States of America

[§] Air Liquide, Newark, United States of America

KEYWORDS

Scheduling, MILP model, continuous power-intensive processes, energy consumption cost, air separation plant.

ABSTRACT

In this work, a mixed-integer linear programming (MILP) model is presented based on a discrete-time scheduling formulation that allows modeling and optimizing operational decisions for processes working under time-sensitive energy prices. The main goal is to find an optimal production schedule, over a given time horizon, that satisfies product demand while minimizing total energy cost. This novel formulation, based on a new concept to model the transitions between alternative operating modes, is very efficient and robust. To illustrate the new capabilities of the model, a comprehensive comparison is performed with a previous alternative model. The model is also used to efficiently solve a real-world industrial case study. The obtained results show optimal solutions for the proposed methodology with modest computational effort.

1. Introduction

Nowadays, the competitiveness of power-intensive industries is highly tied to their ability to adjust production according to time-sensitive electricity prices. In this context, the dynamic management of electricity demand, also referred to as demand side management (DSM), emerges as an effective approach to improve power grid performance and consumer benefits. Industrial DSM needs efficiently integrating production and energy management, which requires detailed understanding of the production process as well as knowledge about power system economics. Efficient management of complex mechanisms of deregulated electricity markets, which are different from typical commodity markets in the process industries, is essential for exploiting DSM opportunities. Particularly in the process industry, which is a major electricity consumer, DSM is becoming critical for maintaining profitability, as stated in Zhang and Grossmann.[1]

Air Separation Units (ASUs) are a typical example of power intensive processes, where very large electric-power air compressors are needed to reach cryogenic temperatures. Due to the recent volatility in energy markets, there is a significant opportunity to reduce costs by taking advantage of lower electricity price periods. In the recent past, a large number of optimization models have been developed to face challenging scheduling problems arising in the PSE community. Detailed reviews of this area can be found in Méndez et al.[2] and, more recently, in Harjunkoski et al.[3]

Particularly, in the area of detailed production scheduling with power optimization, there have been several important contributions in the last decade. Initially, Castro et al.[4] proposed a novel continuous time scheduling formulation for continuous plants operating under variable electricity cost. In turn, Mitra et al.[5] developed an MILP model for the optimal operational production planning for continuous power-intensive processes that participate in non-dispatchable demand response programs. The MILP model allows an accurate and efficient modeling of transitions between operating modes using a discrete time representation. The model was successfully applied to two different real-world air separation plants that supply to the liquid merchant market, as well as cement plants. One year later, Mitra et al.[6] developed a generalized mode model on a component basis for the optimal scheduling of combined heat and power (CHP) plants under time-sensitive electricity prices. The model is capable of tracking the states of the components in terms of operating modes and transitional behavior. The optimization model was applied to a real-world industrial CHP plant, obtaining up to 20 % of profit increase in comparison to a constant operation of the plant. Artigues et al.[7] proposed a two-step integer/constraint programming approach to solve an industrial case-study involving energy constraints and objectives linked to electric power consumption. More recently, Mitra et al.[8] introduced a multi-scale model for the integrated optimization of investments and operations for continuous power-intensive processes under time-sensitive electricity prices and demand uncertainty. They applied the model to an industrial case study of an air separation plant for deterministic demand as well as stochastic demand. Due to the multi-scale nature of the problem, the resulting MILP problems are very large and hard to solve. Therefore, the authors outlined a hybrid bi-level decomposition algorithm in part II of the paper[9] that was able to reduce the computational time by up to two orders of magnitude compared to the full-space method and by 45–85% compared to a Benders decomposition approach. In turn, Pattison et al.[10] addressed the optimal process operation in fast-changing electricity markets with a novel low-order dynamic models and an air separation process. Zhang et al.[11] developed a general discrete-time model for the scheduling of power-intensive process networks with various power contracts. The proposed model consisted of a process network represented by Convex Region Surrogate models that are incorporated in a mode-based scheduling formulation, for which a block contract model is considered to represent a large variety of commonly used power contracts. Subsequently, Zhang et al.[12] faced the simultaneous optimization of short-term production scheduling and electricity procurement under uncertainty for continuous power-intensive processes. Lately, Zamarripa et al.[13] developed two rolling horizon aggregate scheduling approaches to simultaneously deal with production and distribution for industrial gases supply chains, but this time assuming regulated electricity prices. A very recent comprehensive summary of existing works on planning and scheduling for industrial DSM together with the main mechanisms of electricity markets has been reported in Zhang and Grossmann.[1]

It is clear that even though very significant progress has been made in the optimal operational production planning for continuous power-intensive processes, a highly efficient and systematic solution strategy of large-scale industrial problems is still an unresolved issue. In this paper we propose a conceptually different discrete-time MILP scheduling formulation that is capable of effectively dealing with price fluctuations by optimizing operating decisions for energy intensive processes under time-sensitive electricity prices with modest CPU time. The scheduling problem aims at determining the mode and the production amount of a liquefier at every hour such that a given demand is met at minimal energy cost. Various operational constraints such as feasible transition modes, minimum and maximum residence times, minimum and maximum tank levels, and lower and upper bounds on production rates are also to be considered. In the remaining sections of the paper, the scheduling problem of power intensive processes with time-dependent electricity pricing schemes is first described in Section 2, including a description of the operation of liquefiers of an air separation plant and the alternative energy markets. In Section 3, a novel Process State Transition Network MILP-based model (PSTN) is introduced. An existing alternative MILP model is also presented in this section for comparison purposes. The resulting formulation is then used to solve multiple cases (Section 4), comparing the computational performance of the novel proposed approach with the existing one. On the basis of the numerical experiments, conclusions are drawn, and suggestions for further research are made in Section 5.

2. Problem Statement

2.1. Power-Intensive Processes Scheduling

The scheduling problem addressed here focuses on the efficient operation of industrial power-intensive processes. These processes may comprise a set of units. In Section 2.2 we introduce a specific case study related to a liquefier producing a single product (e.g. liquid nitrogen) where the production planning is adjusted to time-dependent electricity pricing schemes.

Due to the significant energy consumption of liquefiers, a key factor that influences the operating decisions is the energy price volatility.[6,14] Electricity can be purchased from the power grid by using alternative power contracts. The different types of markets and how they may differ in price and availability are described in Section 2.2. In particular, in this work we assume that the plant participates in the day-ahead market. Electricity price forecasts for the following days on an hourly time grid $h \in H$, are available to us.

Given electricity price and demand forecasts, a set of operating constraints, such as minimum and maximum production rates based on the plant state, storage capacities of the plant, and minimum final tank inventory, the problem is to determine a production schedule that minimizes the total energy cost while meeting the demand for a given time horizon. Note that the demand can fluctuate on an hourly, daily or weekly basis. The main objective is to find the optimal production schedule that defines operating modes, production and inventory levels.

2.2. Air Separation Plant

Continuous power-intensive air-separation processes use air from the atmosphere and electric energy. The air is compressed and dried for cryogenic separation to obtain industrial gases according to the required specifications of quality.

The composition of dry air is predominantly 78% nitrogen, 21% oxygen, and 1% argon by volume. A main compressor is used to compress air from atmospheric pressure to elevated pressure. Additional compression followed by expansion can supplement the main air compressor, providing extra refrigeration to produce liquid and/or high pressure products. After compression, air is cooled down and partially liquefied in the main heat exchanger. The partially-condensed air enters a cryogenic distillation column, where is separated into its basic components. The huge electricity power used to drive the compression equipment to produce gaseous and liquid air-gases (nitrogen, oxygen and argon), is the largest single operating cost in this process.

At certain plants, the nitrogen gaseous stream can be sent to a liquefier cycle, where the gas is cooled down to liquid phase. Liquefiers typically consist of a feed compressor, a recycle compressor, an expansion turbine booster, a heat exchanger and a separator. For the rest of the paper, we will focus only on the optimal operation of an external liquefier as an example to test the performance of the models. Furthermore, we discuss different operating modes for the feed and recycle compressors and the possible transitions that may occur between them. Figure 1 shows a schematic representation of the feasible configurations and allowed transitions. There are five possible operating modes considered in this illustrative example:

start-up operation: three operation modes are used to model the start-up procedure: "Ramp-up compressor A - Phase I", "Ramp-up compressor A - Phase II", and "Ramp-up compressor B". The liquefier must follow strict ramp-up transitions respecting a minimum residence time in each mode of 1 hour in order to switch from modes "off" to "on". Note that the start-up operation can only be performed after the liquefier stays in the “off” mode for at least a certain time periods.

- *shut-down operation*: Contrary to the start-up procedure, after the liquefier remains in the "on" mode longer than a given lapse of time, it can start the shut-down procedure. Ramp-down characteristics are modeled using the following operation points: "Ramp-down compressor A - Phase I", "Ramp- down compressor A - Phase II", and "Ramp- down compressor B". The duration of each transition mode involved is 1 hour.
- *normal operation (on operation)*: the liquefier is up and running. Once the liquefier has remained in this state during a minimum amount of time (3 hours in our example), a transition may occur to a different mode. Hence, it can switch from "on" to "stand-by" mode immediately, or from "on" to "off" mode following the shut-down procedure described above.
- *stand-by operation*: the liquefier can transition from normal operation to stand-by mode after its minimum stay time is satisfied. Once in stand-by, this configuration must also be

maintained for a minimum stay time (3 hours for the example). The stand-by mode does not include any level of production. In the plant, it is usually used for short stops due to inventory restrictions. In this way, turning the compressors off and on in a short time is avoided.

- *off operation*: the liquefier is entirely shut-down and must remain in the “off” mode for a specified minimum time before it can be started-up. According to Figure 1 the start-up procedure must be performed through an "on-off" transition mode. In this particular example, the "off", "on" and "stand-by" modes have a minimum time residence of 3 hours. However, this time may vary depending on the configuration.

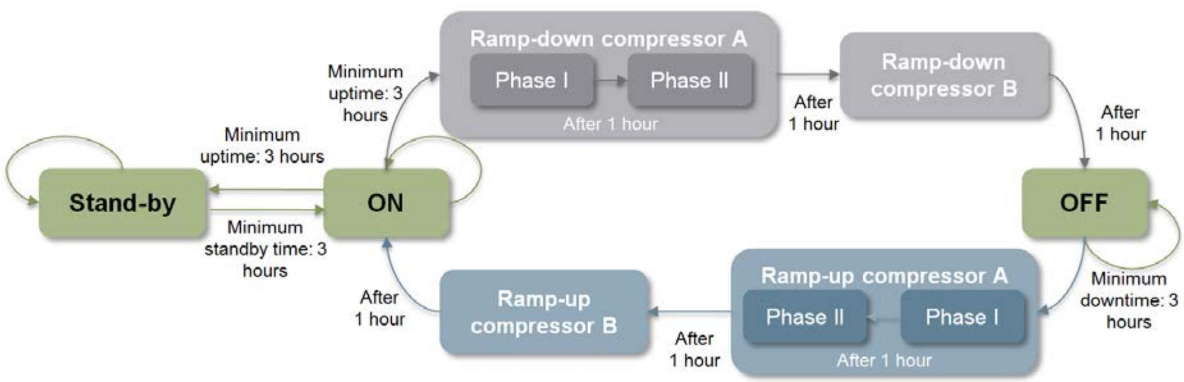

Figure 1. A state graph of the feed and recycle compressors of external liquefier cycle

Note that a transition between alternative operating modes represents how the liquefier changes from one operating point to another. An important aspect in this problem is to consider that the system has operating modes with different minimum durations: 1 hour (ramp-up and ramp-down times) and 3 hours (uptime, standby time, and downtime). Therefore, any deviation from expected operation will affect several time periods. In addition, in some plants there are some constraints concerning both the minimum and maximum residence time of operating modes, such as "on", "off", and "stand-by" modes.

The air separation plant under study is assumed to be able to purchase energy in the day-ahead market, in which the nominations are decided from the expected production for the next day. We assume that forecasts of energy prices are available for the day-ahead market for the next nine days. Later, we propose a novel systematic way of representing the transitory state of the system between modes.

3. Model Formulation

In this section, we present a mathematical formulation of the scheduling problem that corresponds to a mixed integer linear programming problem (MILP). The model developed comprises several components that deal with features of the problem mentioned in previous section, and serves as a fundamental tool to achieve the production schedule that minimizes the total energy cost over a given time horizon.

Although different continuous time models have been effectively used for multiple production scheduling problems with energy constraints,[15-19] given the specific operational restrictions and time characteristics required in this problem, a discrete time representation is used in this paper. It should be noted that discrete-time formulations are better under hourly or smaller changing electricity prices. However, if consecutive hours with the same price or seasonal variations in electricity prices are considered, continuous-time formulations become, in some cases, competitive. In the problem addressed, the scheduling horizon is divided into fixed intervals of time of equal length. Each of these intervals is represented by a period with the length of one hour. According to the selected time discretization a scheduling horizon of a week is considered. Therefore, it consists of 168 periods (hours) and is defined by the set of time periods $T = \{1, 2, \ldots, FT\}$ (see Nomenclature section).

A novel network to systematically represent the scheduling of a process with operating modes and transitions is presented in Section 3.1. A list of indexes, sets, parameters, and variables are detailed in the Nomenclature section and operational constraints are described in Section 3.2. Note that all continuous variables such as power consumption, production and inventory levels in this model are constrained to be nonnegative.

3.1. Process State Transition Network

We propose an explicit modeling formulation of feasible operational transitions and a systematic way of representing the transition states, denoted as the Process State Transition Network (PSTN). Figure 2 shows this novel concept where the feasible transitions between operational states are represented by directed arcs reflecting the process dynamics. In addition, each node (denoted by rectangles) represents a specific transitional state of the liquefier cycle according to the state graph (Figure 1). Note that both nodes and arcs involve operational constraints which must be satisfied at all times.

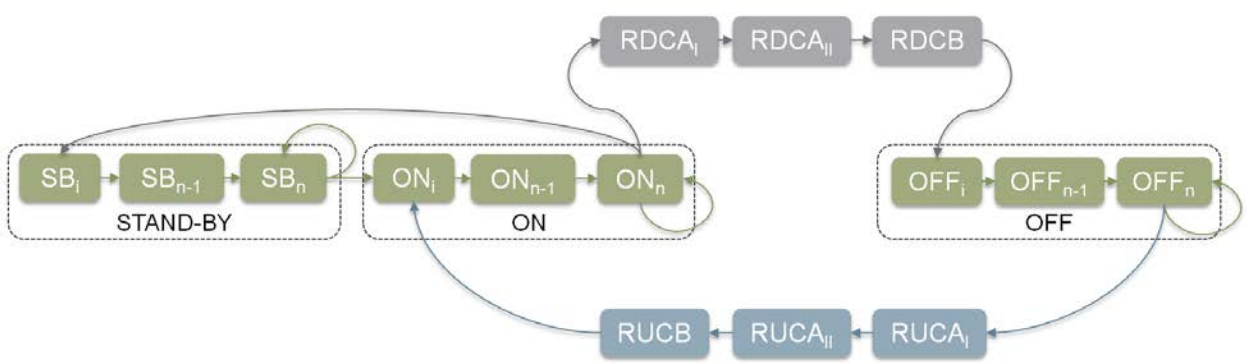

Figure 2. Process State Transition Network

We introduce operational or transitional "states" corresponding to possible operating points of the system. This concept allows the disaggregation of operation modes and a more detailed modeling of the transitional behavior. For instance, states with minimum duration of 3 hours are decomposed in 3 sub-states of 1 hour each and are called initial sequential transition states, intermediate transition states, and critical transition states, respectively. This decomposition occurs in stand-by, on and off operating states in which the liquefier can remain 3 or more hours. Consequently, the main methodological contribution of the proposed paper is the disaggregation of the transition process from one mode to another into a predefined discrete-time operation states. This disaggregation allows to represent the scheduling problem in a conceptually different way with fewer binary variables and simpler constraints compared to previous models

Due to the fact that air-separation processes are power-intensive and are exposed to time-sensitive energy markets, the plant undergoes a dynamic switching behavior.[6,14] Note that an operational constraint imposes the minimum amount of time the any piece of equipment should be running in the same operation mode. There are transitions between different operating states or to the same state. For instance, the liquefier should be off in periods of high prices, provided that demand and minimum final tank level constraints are satisfied. Once the system remained in the off state for at least 3 hours, i.e. transitioned through the OFF_i, OFF_{n-1}, and OFF_n states, it can start to operate according to the states sequence of the start-up phase with a fixed duration of 1 hour in each: $RUCA_I$, $RUCA_{II}$, and $RUCB$.. Consequently, after 3 hours (of the start-up procedure) the liquefier will operate in normal production mode for at least 3 hours.

Nomenclature

Sets

T(index t)	the set of time periods
S(index s)	the set of operating states
D(index d)	the set of days of a week
T^{last}	the subset of ending times of each day
$S^{initial}$	the subset of initial sequential states of On, Off and Stand-by state

S^{inter}	the subset of intermediate transition states of On, Off and Stand-by modes
$S^{critical}$	the subset of critical transition states of On, Off and Stand-by modes
$S^{down-initial}$	the subset of initial state to ramp-down
$S^{up-initial}$	the subset of initial state to start-up
$S^{down-inter}$	the subset of intermediate states to ramp-down
$S^{up-inter}$	the subset of intermediate states to start-up
$S^{minProd}$	the subset of states with minimum production
LIC_s	the subset of states that immediately precedes a critical state s
NTS_s	the subset of states that immediately succeeds critical state s

Parameters

$MinP_s$	minimum production per hour in each state
$MaxP_s$	maximum production per hour in each state
$MDTL_{T^{last}}$	minimum final tank levels at the end of the day
ED_t	expected hourly demand
FPC_s	fixed power consumption
VPC_s	variable power consumption
EP_t	energy price forecast at time t
$Qmin$	minimum Tank Level
$Qmax$	maximum Tank Level
EP^{FIXED}	average energy price of a week
I_0	initial tank level
FT	final time of the scheduling horizon
nd	number of intermediate states in the shutdown process

ns	number of intermediate states in the startup process
min_{res}	minimum residence time
max_{res}	maximum residence time
mn	minimum residence time in critical transition states
mx	maximum residence time in critical transition states
inc	percentage of ramp-up production changes
dec	percentage of ramp-down production changes

Continuous Variables

$P_{s,t}$	production amount at time t for state s
PW_t	power consumption at time t
I_t	inventory available at the end of time period t
$Cost$	total energy cost

Binary Variables

$W_{s,t}$	indicates whether system operates in state s during time period t

3.2. Operational Representation

The MILP-based scheduling formulation requires modeling of a set of constraints to represent the new state graph shown in Figure 2. The PSTN model includes constraints regarding operational decisions, such as production and inventory levels, demand constraints, operating modes and transitions constraints, timing constraints, and energy balance constraints. Additionally, the energy consumption is computed to minimize the total energy cost associated.

We introduce the binary transitional variable $W_{s,t}$ to indicate in which state s the system is operating at time period t ($W_{s,t} = 1$).

Next, we present a set of constraints to satisfy the start-up and shut-down requirements, residence times, mass balance, and constraints concerning power consumption according to time-dependent electricity pricing schemes.

3.2.1. Operation Modes

As shown in the Nomenclature section, the different operating states s in which the system can be operating are defined by the set $(s \in S)$. Since the liquefier has to operate in a single state each hour, constraint (1) forces it to select a single production mode at each time period by using the binary variable $W_{s,t}$.

$$\sum_s W_{s,t} = 1 \qquad \forall t \in T \tag{1}$$

3.2.2. Sequential Transition States

The operating modes are discrete decisions which correspond to the state of the plant or a set of equipment. According to the PSTN network in Figure 2, transitions between states can occur provided that they are executed in the correct order. In other words, there are pre-defined sequences of operation states that describe the switching behavior of the liquefier.

Constraints (2) and (3) represent the operating sequence at on, off or stand-by states. If the operating point of the liquefier in the time period t is in the initial state of on, off or stand-by mode, then at time $t+1$ and $t+2$ the liquefier has to operate in the corresponding states, intermediate and critical, respectively.

$$W_{s,t} = \sum_{s' \in S^{inter}} W_{s',t+1} \qquad \forall t \in T, s \in S^{initial} \tag{2}$$

$$W_{s,t} \leq W_{s',t+1} \qquad \forall t \in T, s \in LIC_s, s' \in S^{critical} \tag{3}$$

The start-up and shut-down procedures may not be interrupted. Consequently, during these processes the liquefier has to comply with given transition sequences of states through 3 different states which have the same residence time (1 hour). The feasible sequences $off \rightarrow startup \rightarrow$

on and $on \rightarrow shutdown \rightarrow off$ are effectively guaranteed by constraints (4) and (5), respectively. For instance, if the liquefier is turned off, it cannot be turned on directly due to the fact that the start-up procedure must be satisfied. Hence, the specific sequence of transition states corresponding to that process is modeled by consuming 1 hour in each state: $RUCA_I$, $RUCA_{II}$, and $RUCB$.

$$nd * W_{s,t} = \sum_{s' \in S^{down-inter}} \sum_{t'=t+1}^{t'=t+nd} W_{s',t'} \qquad \forall t \in T, s \in S^{down-initial} \tag{4}$$

$$ns * W_{s,t} = \sum_{s' \in S^{up-inter}} \sum_{t'=t+1}^{t'=t+ns} W_{s',t'} \qquad \forall t \in T, s \in S^{up-initial} \tag{5}$$

However, additional constraints are necessary to complete the switching between the on and off states. Constraints (6) and (7) model the last state transition required to switch from on to off state, and vice versa, respectively.

$$W_{RDCB,t} = W_{OFF_i,t+1} \qquad \forall t \in T \tag{6}$$

$$W_{RUCB,t} \leq W_{ON_i,t+1} \qquad \forall t \in T \tag{7}$$

In contrast to the OFF_i state, the ON_i state (first sub-state of on operating point) has two possible previous states (see Figure 2): SB_n and $RUCB$. Therefore, constraint (6) is represented by an equality and constraint (7) by an inequality. Additionally, constraint (8) is also defined to represent these two feasible paths to ON_i state. For instance, if the liquefier is operating in the first hour of the on mode (ON_i state) at time t, it means that, according to the feasible transitions represented in Figure 2, the liquefier may have been in SB_n or $\boldsymbol{RUCB}$ state at time $t-1$. This transition is represented below.

$$W_{SB_n,t} + W_{RUCB,t} \geq W_{ON_i,t+1} \qquad \forall t \in T \tag{8}$$

3.2.3. Critical Transition States

Once the system operates in a critical state (ON_n, OFF_n, and SB_n) in the period t, it can remain in the same state or switch to other in the next period ($t+1$). To describe possible transitions that can occur from the critical states constraint (9) is formulated. The binary variable $W_{s,t}$ is used to meet the allowed switches**.** For example, when the liquefier operates in ON_n state at time $\boldsymbol{t}$**,** then in time period $t+1$ it can operate in $\boldsymbol{SB_i}$, $\boldsymbol{RDCA_I}$ or stay in ON_n state.

$$W_{s,t} + W_{s\prime,t} = \sum_{s\prime\prime \in NTS_s} W_{s\prime\prime,t+1} \qquad \forall t \in T, s \in S^{critial}, s' \in LIC_s \tag{9}$$

Furthermore, the transition between an intermediate state and a critical state belonging to the same operating mode (on, off or stand-by) is also modeled by enforcing constraint (9). Note that the liquefier can operate only in one state every hour, so only a binary variable on each side of the equality can be activated.

3.2.4. Residence Time Constraints

The liquefier has both minimum and maximum stay constraints which enforce lower and upper bounds on the residence time of particular operation modes. These constraints become active when there is a transition involved, depending on the previous liquefier configuration. More precisely, after a start-up or shut-down procedure is performed, i.e. a transition occurs to state ON_i or OFF_i, respectively. Then, the liquefier has to remain in that state at least a given minimum residence time. At the same time, the liquefier cannot remain in the same mode for a longer period than a specified time.

To ensure the minimum and maximum residence times we formulate constraints (10)-(13), which are applied to those modes with more than one hour of minimum residence in: on, off, and stand-by states.

3.2.4.1. Minimum Residence Time

Note that there is an operational constraint on the minimum amount of time that the liquefier should remain in the same mode. Whenever the liquefier switches to a different operation state, the action will affect several time periods, i.e. 3 hours for the suggested example. Therefore, we introduce constraint (10) to model this minimum number of hours min_{res}, in which the liquefier is required to stay in a certain mode.

$$mn * W_{s,t} = \sum_{s' \in S^{critical}} \sum_{t'=t+1}^{t+mn} W_{s',t'} \qquad \forall t \in T, s \in S^{inter}: t \leq (FT - mn) \qquad (10)$$

where mn represents the number of time periods that the liquefier must operate in the critical transition state (the last sub-mode of on, off or stand-by modes) to satisfy the minimum residence time. This state must be repeated for mn hours after a transition from another state occurred. Only then, the system configuration can switch from the critical transition state to any of the states belonging to the corresponding NTS_s. It is important to note that the initial and intermediate transition sub-states last only one hour. Thus, mn is calculated by using the following equation:

$$mn = min_{res} - 2 \qquad (11)$$

According to Figure 2, constraint (10) can be applied to guarantee the minimum uptime, downtime and stand-by, which are represented by on, off, and stand-by operation states.

3.2.4.2. Maximum Residence Time

Similarly to the minimum residence time constraint, we define constraints (12) and (13) to fix the maximum number of hours max_{res} that the liquefier must operate in particular modes such as on, off or stand-by states. For instance, if the liquefier is switched to off, it cannot stay in this operating point longer than a specified number of hours. Therefore, the liquefier cannot remain more than mx time periods in any critical transition state.

$$\sum_{t'=t}^{t+mx} W_{s,t'} \leq mx \qquad \forall t \in T, s \in S^{critical}: t \leq (FT - max_{res}) \qquad (12)$$

$$mx = max_{res} - 2 \qquad (13)$$

3.2.5. Mass Balance

The following set of constraints defines production rates, inventory levels, and the relationship between them by mass balances. The liquefier operation is required to meet inventory levels for each hour of the planning horizon, taking into account the production levels according to the operating states applied.

3.2.5.1. Production Rate Constraint

The production level of each time period depends on its plant configuration and is denoted by the variable $P_{s,t}$. Each operation state s has a minimum ($MinP_s$) and a maximum ($MaxP_s$) production limits. Hence, the binary variable $W_{s,t}$ is used in constraint (14) to guarantee that production ($P_{s,t}$) will always satisfy the predefined allowed limits, taking into account the liquefier operation state in each hour.

$$W_{s,t} * MinP_s \leq P_{s,t} \leq W_{s,t} * MaxP_s \qquad \forall t \in T, s \in S \tag{14}$$

In addition, production levels cannot abruptly change from one time period to another, i.e. production must gradually vary over time. For instance, if the liquefier goes into the start-up operation at time t, it can start to produce at $t + 3$, but not in its maximum production rate. Due to the fact that there are both strict ramp-up/down production limits, we define two process parameters: inc and dec. The following set of constraints (15)-(17) describe the above ramping behavior (up and down). We assume that the liquefier starts to operate in on state (ON_i) at the minimum production level and varies it as needed.

$$P_{s',t-1} * dec \leq P_{s,t} \leq P_{s',t-1} * inc \qquad \forall t \in T, s' \in S^{initial}, s \in S^{inter} \tag{15}$$

$$\left(P_{s'',t-1} + P_{s',t-1}\right) * dec \leq P_{s,t} \leq \left(P_{s'',t-1} + P_{s',t-1}\right) * inc$$

$$\forall t \in T, s' \in S^{inter}, s \in S^{critial}, s'' \in S^{initial} \tag{16}$$

$$P_{s,t} = W_{s,t} * MinP_s \qquad \forall t \in T, s \in S^{minProd} \tag{17}$$

3.2.5.2. Inventory Constraints

We define the variable I_t which represents the product stored at each time period t according to the amounts produced and consumed by the customers. Thus, a mass balance is formulated by (18) and (19) to express the relationship between these amounts. Both constraints are defined in the time period in which the mass balance is calculated. While the former calculates the inventory in the first hour ($t = 1$) considering the production and demand of that hour, and only the initial inventory of the planning horizon, the latter establishes that the inventory level at the end of time period t ($t > 1$) will be equal to the product inventory at the end of the previous period ($t - 1$), plus the current production level according to the s state, minus the amount delivered at time t.

$$I_t = I_0 + \sum_s P_{s,t} - ED_t \qquad \forall t \in T: t = 1 \tag{18}$$

$$I_t = I_{t-1} + \sum_s P_{s,t} - ED_t \qquad \forall t \in T: t > 1 \tag{19}$$

Note that the demand, denoted by ED_t, is defined on an hourly basis but can also be specified on a daily or weekly basis. Moreover, the maximum ($Qmax$) and minimum ($Qmin$) amount of the inventory allowed in the plant must be satisfied at every time. This inventory level restriction is captured by the following constraint:

$$Qmin \leq I_t \leq Qmax \qquad \forall t \in T \tag{20}$$

3.2.5.3. Final Tank Level Constraint

Finally, the plant has to meet a minimum level of inventory at the end of the planning horizon, corresponding to the last day of the week under review ($FT = 168$). We denote the value of the minimum amount of product stored by $MDTL_{T^{last}}$ and is calculated as follows:

$$I_t \geq MDTL_{T^{last}} \qquad \forall t \in T^{last} \tag{21}$$

3.2.6. Energy Balance Constraints

In order to calculate the amount of power consumed at every time t, we define the variable PW_t and constraint (22). The summation estimates the energy requirements in terms of the fixed FPC_s and the variable power consumption VPC_s. The first of these terms is associated with the operating state of the liquefier at any particular time t, while the second depends on associated production levels .

$$PW_t = \sum_s (W_{st} * FPC_s + VPC_s * P_{st}) \qquad \forall t \in T \tag{22}$$

3.2.7. Objective Function

The objective function aims at minimizing the total energy cost and can be represented by constraint (23). Note that the power consumption calculated in constraint (22) is used as the key factor in the objective function. Hence, the summation (23) computes the power consumption cost for the whole scheduling horizon. The energy price forecast, represented by EP_t, can be specified on an hourly or daily basis, or a flat energy price can also be used.

$$\text{Min } Cost = \sum_t (PW_t * EP_t) \tag{23}$$

3.3. Alternative Model

An alternative approach proposed by Mitra et al.[5] has been previously reported as an efficient scheduling model to optimize production planning for continuous power-intensive processes. Mitra et al.[5] developed a discrete-time scheduling formulation to determine the production and inventory levels, and the operation modes for each time period according to time-dependent electricity pricing schemes. Their MILP model was also used to evaluate an industrial case study on an air separation plant which produces multiple liquid and gaseous products, such as oxygen, nitrogen, and argon.

The major difference between Mitral et al.[5] model and the PSTN model proposed in this paper is the way to represent the operation points of the plant and to capture the transition mode behavior. While Mitra et al.[5] represent the operational transitions defining global transitional modes m $(m \in M)$ as a set of operating points to capture the transitional behavior of the plant during a specific time period, such as off, ramp-up transition, or on, in the PSTN model disaggregates these operation modes in operational states at each time period.

To model the production modes of the air separation plant, Mitra et al.[5] use the binary variable $Y_{p,m}^{t}$ which is equivalent to the one used in this paper to produce a product, $W_{s,t}$, and also determined the operational mode each hour by equation (1). In addition, they incorporate the continuous variable Pr^{t} to calculate the total production level at each hour t using the following equation:

$$Pr^{t} = \sum_{m \in M} \overline{Pr}_{m}^{t} \qquad \forall t \in T \tag{24}$$

where $\overline{Pr}_{m}^{t}$ represents, as well as $P_{s,t}$, the production level of each operational point of the plant. Note that both $MaxP_{s}$ of our model and $\bar{M}_{m}$ of constraint (25) by Mitra et al.[5] represent the maximum production.

$$\overline{Pr}_{m}^{t} \leq \bar{M}_{m} * Y_{m}^{t} \qquad \forall m \in M, t \in T \tag{25}$$

As a major key difference, Mitra et al.[5,6] introduced the binary transitional variable $Z_{m',m}^{t}$, which is true whenever a transition from mode m' to mode m occurs from time period $t-1$ to t. In order to reduce the number of switching constraints proposed by Mitra et al.,[5] Mitra et al.[6] reformulated them by obtaining constraint (26).

$$\sum_{m' \in M} Z_{m',m}^{t} - \sum_{m' \in M} Z_{m,m'}^{t} = Y_{m}^{t} - Y_{m}^{t-1} \qquad \forall t \in T, m \in M \tag{26}$$

As shown in Mitra et al.,[6] constraint (27) was defined to model the minimum stay. Note it is a modification of the constraint presented in Mitra et al.[5] In addition, they used the transitional mode constraint (28) and constraint (29) for forbidden transitions. Note that both $K_{m,m'}^{min}$ and min_res represent the same value.

$$Y_{m'}^{t} \geq \sum_{\theta=0}^{K_{m,m'}^{min}-1} Z_{m,m'}^{t-\theta} \qquad \forall (m,m') \in Seq, t \in T \tag{27}$$

$$Z_{m,m'}^{t-K_{m,m'}^{min}} - Z_{m',m''}^{t} = 0 \qquad \forall t \in T, (m,m',m'') \in Trans \tag{28}$$

$$Z_{m,m'}^{t} = 0 \qquad \forall t \in T, (m,m') \in DAL \tag{29}$$

Finally, the mass balance of the plant is modeled by equations (20) and (30), where the latter is equivalent to equation (19) used in this paper.

$$I_t + Pr^t = I_{t+1} + ED_t \qquad \forall t \in T \tag{30}$$

4. Numerical Experiments

The computational efficiency of the proposed model was tested in a liquefier cycle that can be typically found at air separation plants. Real-world electricity prices, setups, and demand input data for a weekly horizon (168 hours) were taken into account. Next, we describe the application of our model formulation to this case study, presenting the real industrial data used to generate different scenarios and numerical results. Moreover, we show a comprehensive computational comparison between the proposed optimization model and the one developed by Mitra et al.[5] Finally, we calculate the economic impact of the PSTN model by optimizing different plant configurations.

4.1. Case Study Definition

In this section we apply the proposed modeling framework introduced above and illustrated in Figure 2 to the liquefier cycle of an air separation plant of our case study. The data used to test the computational performance of the PSTN formulation is given below. Input data concerning both the minimum and maximum production levels and the power consumption are given in

Table 1 and defined for each operating mode. For confidentiality reasons the corresponding data has been normalized. Note that FPC_s and VPC_s values correspond to the fixed and variable power consumption parameters, respectively, and are used to calculate the power consumption according to equation (22).

Table 1. Production rates and power consumption for the different operating modes

		Mode On	Mode Off	Mode Standby	Ramp-down compressor A		Ramp-down compressor B	Ramp-up compressor A		Ramp-up compressor B
					Phase I	Phase II		Phas e I	Phase II	
Minimum Production [unit/h]		0.8	0	0	0.8	0.8	0.8	0	0	0
Maximum Production [unit/h]		1	0	0	1	1	1	0	0	0
Power Consumption* [MWh/unit]	FPC_s	0	0	1.1	0.63	0.7	2.41	0.36	0.6	3.1
	VPC_s	11.25	0	0	11.25	11.25	11.25	0	0	0

*Power consumption follows a linear correlation: $PW_t = \sum_s (W_{st} * FPC_s + VPC_s * P_{st})$, $\forall t \in T$.

The daily demand data, which have also been normalized, can be found in Table 2. Furthermore, the storage capacity in the plant can vary between 34 and 87 [unit], which represent $Qmin$ and $Qmax$ parameters, respectively.

Table 2. Expected demand for a week [unit/day]

	Expected Demand
Monday	11.3
Tuesday	13.9
Wednesday	14.1
Thursday	13.2
Friday	11.0
Saturday	5.7
Sunday	5.8
Weekly demand	75

We consider two typical weeks of the day-ahead market for electricity price forecast (Forecast 1 and Forecast 2) which are shown in Figure 3. It is important to highlight that both demand levels and energy prices forecasts used in our case study are provided on an hourly basis over a weekly horizon. Hence, the input data regarding the expected demand (Table 2) is disaggregated on an hourly basis to generate the demand scenarios.

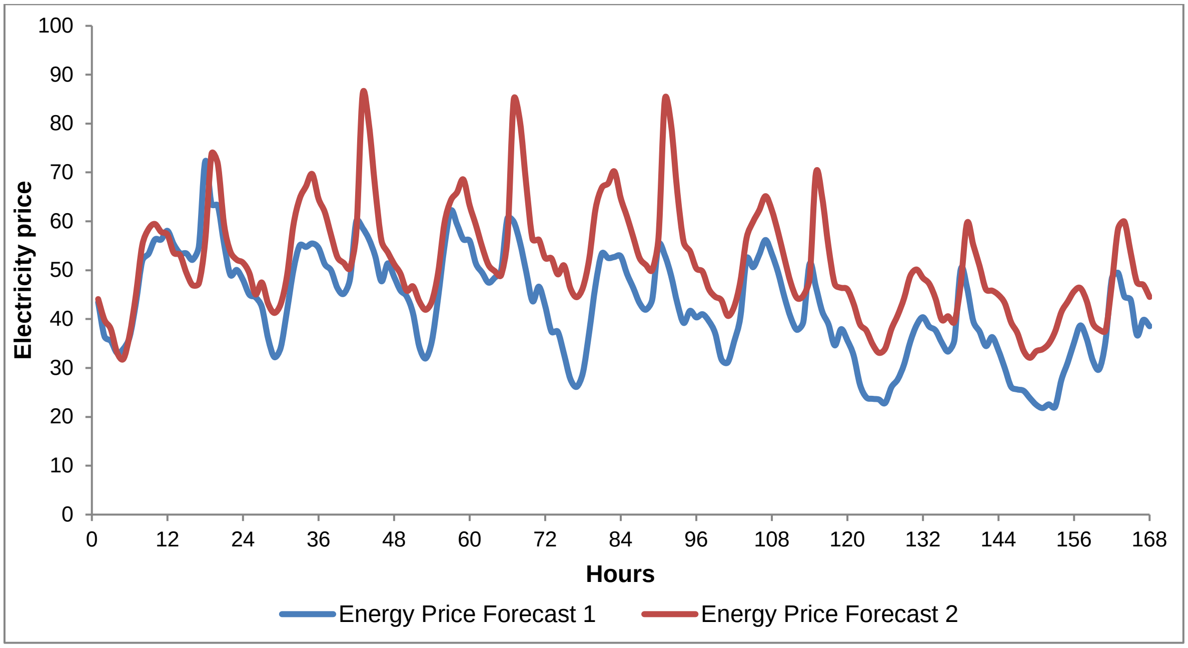

Figure 3. Energy Price Forecasts for two different weeks [$/MWh]

4.2. Computational Statistics

4.2.1. Comparison with Alternative Model

First, we compare the computational efficiency of our model with that of the model presented by Mitra et al.[5] In order to obtain comparable results, we implemented both models in the same computational environment under same assumptions that are reported in the model formulation by Mitra et al.[5] Therefore, ramping down/up constraints were not taken into account in this comparison.

We analyzed six cases (1-6) which are defined according to three expected demand levels and two electricity price forecasts, given in Table 3. The liquefier configuration evaluated considers 3 and 8 hours of minimum and maximum residence time, respectively. In all cases, the calculation of the objective function for both models is performed with equation (23) that computes the total energy cost necessary for normal operation.

Table 3. Case studies based on demands and energy price forecasts

Case*	Demand [unit/day]	Energy Price Forecast
1	Expected Demand	Forecast 1
2	Expected Demand + 15%	Forecast 1
3	Expected Demand - 15%	Forecast 1
4	Expected Demand	Forecast 2
5	Expected Demand + 15%	Forecast 2
6	Expected Demand - 15%	Forecast 2

* Minimum residence time: 3 hours. Maximum residence time: 8 hours.

It is important to remark that the termination criterion was either 0 % optimality gap or 3600 sec of CPU time. The solutions were obtained with the commercial solvers CPLEX 12.6.3.0 and Gurobi 6.5.2 on a PC Intel Xeon X5650 2.6 GHz. The optimization environment employed to solve all test cases was GAMS 24.7.6.

The computational statistics and results of six cases using CPLEX are reported in Table 4 in which the optimal objective has been normalized. It can be observed that the MIP solutions for Cases 2-4 and Case 6 are the same for both models. However, Mitra et al.[5] cannot reach optimality in the maximum predefined CPU time. In Case 1 and 5, the optimal solution is reached by the novel MILP model in less than 16.4 sec, while Mitra et al.[5] can provide only a feasible result with 2.52 % and 1.74 % relative gap in 3600 CPUs, respectively. Hence, all cases solved using PSTN model reached the desired level of optimality in less than 30 sec while most cases cannot guarantee optimality in less than 1 hour by using the model developed by Mitra et al.[5]

Note also that the problem sizes differ clearly. Mitra et al.[5] has fewer continuous variables than the PSTN model, but, it has more equations and practically twice the number of binary variables. Moreover, the solutions of the relaxed mixed integer programming problem (RMIP) for our model were closer to the MIP solutions. In turn, Table 5 reports a comprehensive comparison of the computational performance of the Mitra et al.[5] model using different optimization codes and relative gap values. Although we can observe a better computational behavior when the Gurobi solver is used, the performance is still worst in comparison with the novel PSTN MILP formulation. On the basis of all these cases, we can conclude that our MILP model is computationally much more efficient than the MILP model previously presented by Mitra et al.[5] In effect, one of the major contributions of this work is to remark the fact that although both formulations are based on a discrete time representation, using a more efficient and direct modeling of key problem decisions and constraints can make a remarkable difference in terms of computational performance and solution quality.

Table 4. Comparison of PSTN MILP model with Mitra et al.[5] Model

Case	PSTN Model							Mitra et al.[5] Model						
	Binary vars	Continuous vars	Constraints	RMIP solution	MIP solution	Relative GAP	CPU time [sec.]	Binary vars	Continuous vars	Constraints	RMIP solution	MIP solution	Relative GAP	CPU time [sec.]
1	2536	2858	9215	305.3	336.7	0	16.4	4207	1348	13531	299.1	337.2	2.52	3600
2	2536	2858	9215	356.0	387.0	0	15.5	4207	1348	13531	355.8	387.0	1.81	3600
3	2536	2858	9215	253.1	290.3	0	19.0	4207	1348	13531	250.7	290.3	2.60	3600
4	2536	2858	9215	384.8	413.1	0	17.7	4207	1348	13531	381.3	413.1	0.49	3600
5	2536	2858	9215	449.2	473.7	0	5.1	4207	1348	13531	447.1	474.2	1.74	3600
6	2536	2858	9215	321.1	355.7	0	7.5	4207	1348	13531	316.6	355.7	0	2902

Table 5. Computational statistics for Mitra et al.[5] Model with different solvers and relative gap values

Case	Relative GAP=0.05				Relative GAP=0.01				Relative GAP=0			
	CPLEX		GUROBI		CPLEX		GUROBI		CPLEX		GUROBI	
	MIP solution	CPU time [sec.]	MIP solution	CPU time [sec.]	MIP solution	CPU time [sec.]	MIP solution	CPU time [sec.]	MIP solution	CPU Time [sec.]	MIP solution	CPU time [sec.]
1	338.4	414.8	336.8	661.2	336.8	13432.7	336.7	2028.5	336.7	16883.4	336.7	3228.4
2	387.6	345.7	387.0	148.4	387.0	6650.6	387.0	1745.7	387.0	13179.1	387.0	2407.7
3	290.7	1990.7	290.3	672.0	290.6	7037.1	290.3	5202.9	290.3	10460.3	290.3	6965.3
4	416.7	334.2	413.3	124.7	413.4	2257.1	413.1	922.5	413.1	3905.1	413.1	1327.2
5	474.8	54.0	474.4	91.2	473.7	5547.7	473.7	901.7	473.7	8666.1	473.7	1743.2
6	356.0	481.5	355.7	221.2	355.7	2178.7	355.7	976.7	355.7	2902.0	355.7	1152.3

4.2.2. Case Studies

In this section, we study a set of operational configurations to determine experimental results and the economic impact of the MILP model in the objective function ($Cost$). Additionally, the impact of electricity pricing variability in the day-ahead market is analyzed. Cases (A-E) are reported in Table 6, and are based on the input data used for Case 1 (Table 3) considering a one-hour time discretization and one-week time horizon. Thus, the expected demand and the energy price forecast are assumed to be the same for all scenarios. More specifically, scenarios differ in input parameters such as minimum and maximum residence times. The variation of these parameters, the problem sizes, and the computational results can be found in Table 6. Note that all scenarios evaluated were solved using the ramping constraints (15)-(17) to model the ramping behavior (up and down).

Table 6. Computational statistics applying the PSTN Model

Case	Minimum residence time	Maximum residence time	Binary Variables	Continuous Variables	Constraints	MIP solution	Relative GAP	CPU time [sec.]	Liquefier shutdowns

A	3	8	2536	2863	10727	348.4	0	33.57	9
B	3	16	2536	2863	10703	308.7	0	2.51	6
C	3	24	2536	2863	10679	306.4	0	3.42	6
D	8	24	2536	2863	10679	318.4	0	13.35	5
E	16	24	2536	2863	10679	338.4	0	8.14	4

The results show optimal solutions for all cases using the proposed methodology requiring a modest computational effort. We can observe that, as before, all cases can be solved in a few seconds. Therefore, the MILP model does not require more than 1 minute of CPU time to find optimal solutions with zero optimality gap.

It can be seen that for cases B and C, there are no significant differences in performance and results. This can be due to the maximum stay constraint (with 16 and 24 hour, respectively) not being active. Note that if we consider other energy pricing profiles, these results may be modified.

Furthermore, we can demonstrate that the number of transitions decrease as the flexibility of the operational configuration is increased. This can be reflected in terms of number of liquefier shutdowns and MIP solutions. For instance, case D has a longer residence time allowed than case A. Hence, it involves fewer liquefier shutdowns over the specific time horizon. The required schedules for both tests can be found in Figures 4.a and 4.b.

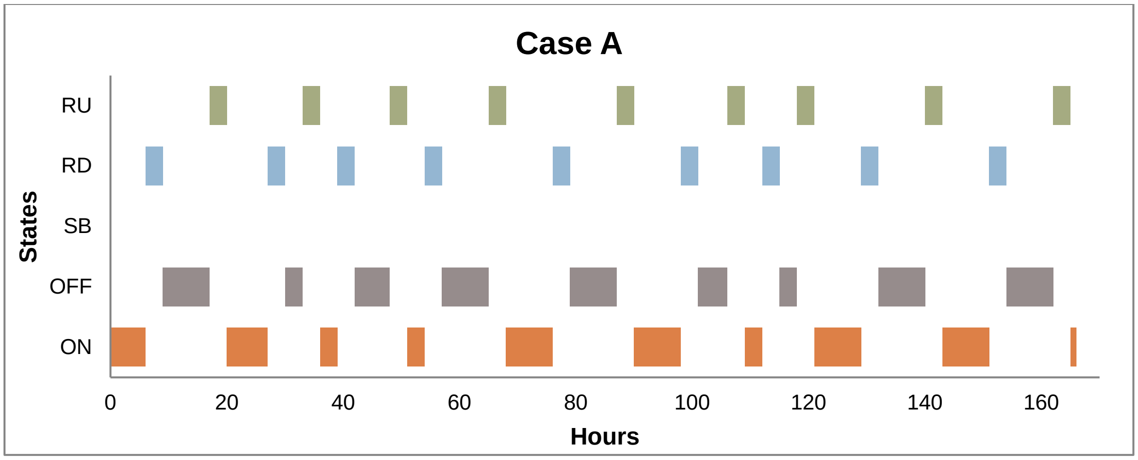

Figure 4.a. Optimal schedule for case A

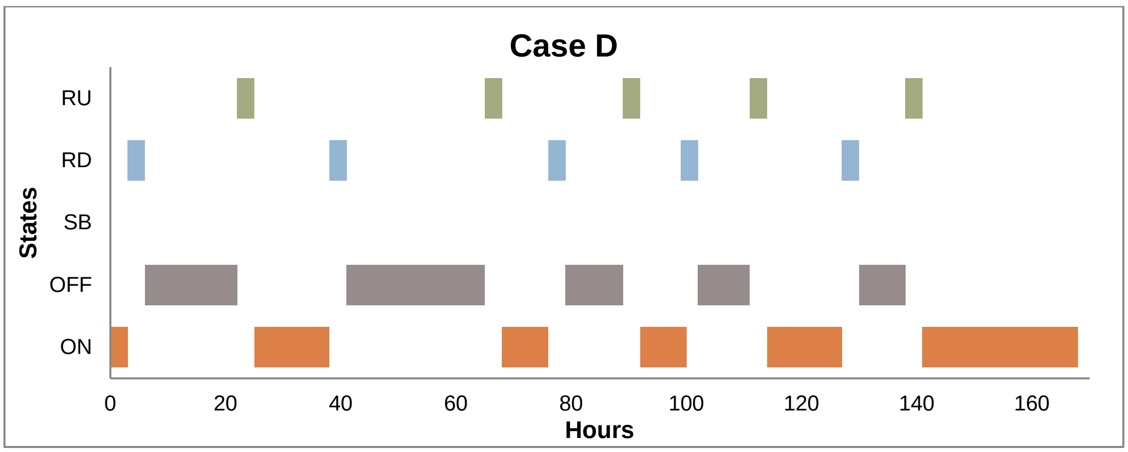

Figure 4.b. Optimal schedule for case D

For the same demand profile, the total energy costs differ according to the different stay restrictions in critical states. The improvements concerning energy costs occur due to the fact that the liquefier operates at its maximum rate during the lowest energy prices, and switches off during the hours of peak prices. To illustrate this behavior, we show the results obtained for case A and case D in Figure 5, in terms of relative power consumption and electricity pricing (Forecast 1). A lower total energy cost in case D than in case A can be observed. Case D uses less energy due to the fact that it needs fewer liquefier shutdowns and its maximum residence time allows it to operate more extensively in periods of low prices.

The highest levels of energy consumption of these cases were the hours of the day with lowest prices, typically by the end of week. Hence, the amount of energy consumed was optimized by using the PSTN formulation to meet demand and operational restrictions.

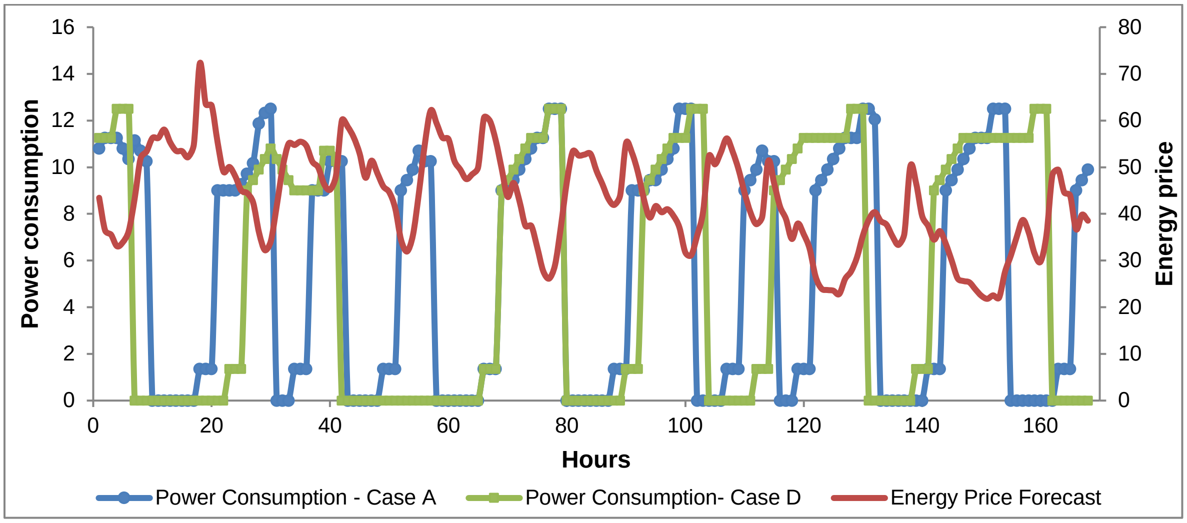

Figure 5. Power consumption profiles for cases A and D

We also compare both cases with regard to their corresponding inventory profiles and production levels. We illustrate these profiles in Figure 6, such as the lower and upper bound of the storage capacity. It can be seen that the inventory level is increased in time periods in which the liquefier operates, and therefore has normal production. Similarly, the amount of stored product decreases in the hours where there is no production, i.e. during liquefier shutdowns, because demand can be met with inventory. Moreover, despite of both storage tank profiles satisfying the minimum and maximum tank levels, case A presents higher inventory levels throughout the planning horizon.

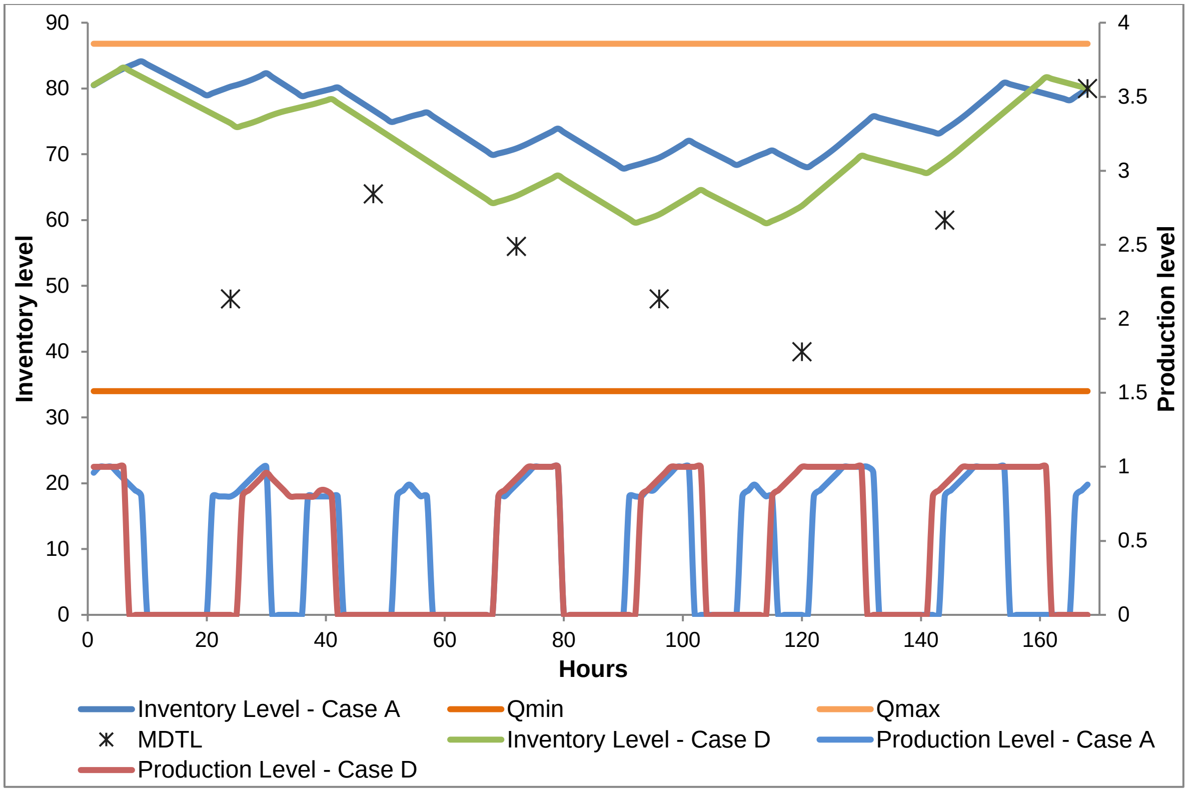

Figure 6. Inventory and production profiles for cases A and D

5. Conclusions

In this paper we have proposed a discrete-time scheduling formulation based on a MILP model that is capable of effectively dealing with price fluctuations by optimizing operating decisions for energy intensive processes under time-sensitive electricity prices. We developed the novel PSTN formulation to systematically represent the operating states and to model the dynamic transition behavior of this type of processes. The major advantage of PSTN is that it gives rise to a discrete-time scheduling formulation that is slightly tighter and computationally superior to previous MILP models.

The main goal of the proposed model is to minimize total energy cost while product demand satisfaction is guaranteed accounting for volatile nature of the energy markets. Thus, it allows the evaluation of daily and hourly reactive decisions based on energy price changes. We were able to successfully implement the model and evaluate multiple instances for an industrial case study. The results established that despite the large size of the MILP model with thousands of constraints and binary and continuous variables can be solved in only few seconds. More precisely, we observed that the optimization model was able to obtain the optimal solution with 0% gap solution for all test cases in less than one minute CPU time.

Furthermore, for different baseline demands and energy price forecasts, we compared the computational requirements of the PSTN model with the formulation previously presented by Mitra et al.[5] The comparison performed demonstrated that the proposed model consistently outperforms the previous one. Based on the results for different optimality gaps, it can be concluded that the novel PSTN MILP-based scheduling model is computationally very efficient and robust for solving real-world industrial scheduling problems. In effect, a central achievement of this work is to clearly illustrate the fact that alternative discrete time MILP formulations may have a remarkable difference in terms of computational performance and solution quality depending on the basic ideas that are used in each model. Based on its high computational performance, the new model can be easily extended to rescheduling of extremely dynamic production environments. Therefore, the proposed scheduling framework is a promising approach for the application to real-world air separation industrial plants. At the same time, the PSTN model can be easily adapted to other operational configurations to find the optimal schedule in a reasonable computational time.

As future work we plan to extend the proposed efficient deterministic formulation to deal with multiple products, i.e. oxygen and nitrogen. Also, incorporating main PSTN model ideas to a novel framework based on stochastic programming or robust optimization to address uncertainty in electricity price data.

ACKNOWLEDGMENT

The authors gratefully acknowledge the financial support received from Air Liquide for conducting research in this project, from CONICET under Grant PIP 112 20150100641 and from ANPCYT under Grant PICT-2014-2392.

REFERENCES

(1) Zhang, Q.; Grossmann, I. E. Enterprise-wide Optimization for Industrial Demand Side Management: Fundamentals, Advances, and Perspectives. *Chem. Eng. Res. Des*. **2016**, *116*, 114.

(2) Méndez, C. A.; Cerdá, J.; Grossmann, I. E.; Harjunkoski, I.; Fahl, M. State-of-the-art Review of Optimization Methods for Short-term Scheduling of Batch Processes. *Comput. Chem. Eng.* **2006**, *30*(6-7), 913.

(3) Harjunkoski, I.; Maravelias, C. T.; Bongers, P.; Castro, P. M.; Engell, S.; Grossmann, I. E.; Hooker, J.; Méndez, C.; Sand, G.; Wassick, J. Scope for Industrial Applications of Production Scheduling Models and Solution Methods. *Comput. Chem. Eng.* **2014**, *62*, 161.

(4) Castro, P. M.; Harjunkoski, I.; Grossmann, I. E. New Continuous Time Scheduling Formulation for Continuous Plants Under Variable Electricity Cost. *Ind. Eng. Chem. Res*. **2009**, *48*(14), 6701.

(5) Mitra, S.; Grossmann, I. E.; Pinto, J. M.; Arora, N. Optimal Production Planning Under Time-sensitive Electricity Prices for Continuous Power-Intensive Processes. *Comput. Chem. Eng*. **2012**, *38*, 171.

(6) Mitra, S.; Lige, S.; Grossmann, I. E. Optimal Scheduling of Industrial Combined Heat and Power Plants Under Time-sensitive Electricity Prices. *Energy*. **2013**, *54*,194.

(7) Artigues, C.; Lopez, P.; Haït, A. The Energy Scheduling Problem: Industrial Case-study and Constraint Propagation Techniques. *Int. J. Prod. Econ*. **2013**, *143*, 13.

(8) Mitra, S.; Pinto, J. M.; Grossmann, I. E. Optimal Multi-scale Capacity Planning for Power-intensive Continuous Processes Under Time-sensitive Electricity Prices and Demand Uncertainty. Part I: Modeling. *Comput. Chem. Eng*. **2014**, *65*, 89.

(9) Mitra, S.; Pinto, J. M.; Grossmann, I. E. Optimal Multi-scale Capacity Planning for Power-intensive Continuous Processes Under Time-sensitive Electricity Prices and Demand Uncertainty. Part II: Enhanced Hybrid Bi-level Decomposition. *Comput. Chem. Eng*. **2014**, *65*, 102.

(10) Pattison, R.C.; Touretzky, C.R.; Johansson, T.; Harjunkoski, I.; Baldea, M. Optimal Process Operations in Fast-changing Electricity Markets: Framework for Scheduling with Low-order Dynamic Models and an Air Separation Application. *Ind. Eng. Chem. Res*. **2016**, *55*(16), 4562.

(11) Zhang, Q.; Cremer, J. L.; Grossmann, I. E.; Sundaramoorthy, A.; Pinto, J. M. Risk-based Integrated Production Scheduling and Electricity Procurement for Continuous Power-intensive Processes. *Comput. Chem. Eng*. **2016**, *86*, 90.

(12) Zhang, Q.; Sundaramoorthy, A.; Grossmann, I. E.; Pinto, J. M. A discrete-time Scheduling Model for Continuous Power-intensive Process Networks with Various Power Contracts. *Comput. Chem. Eng*. **2016**, *84*, 382.

(13) Zamarripa, M.; Marchetti, P. A.; Grossmann, I. E.; Singh, T.; Lotero, I.; Gopalakrishnan, A.; Besancon, B.; André, J. Rolling Horizon Approach for Production−Distribution Coordination of Industrial Gases Supply Chains. *Ind. Eng. Chem. Res*. **2016**, *55*(9), 2646.

(14) Karwan, M. H.; Keblis, M. F. Operations Planning with Real Time Pricing of a Primary Input. *Comput. Oper. Res*. **2007**, *34*, 848.

(15) Nolde, K.; Morari, M. Electrical Load Tracking Scheduling of a Steel Plant. *Comput. Chem. Eng*. **2010**, *34*, 1899.

(16) Castro, P. M.; Harjunkoski, I.; Grossmann, I. E. Optimal Scheduling of Continuous Plants with Energy Constraints. *Comput. Chem. Eng*. **2011**, *35*, 372.

(17) Haït, A.; Artigues, C. On Electrical Load Tracking Scheduling for a Steel Plant. *Comput. Chem. Eng*. **2011**, *35*, 3044.

(18) Hadera, H.; Harjunkoski, I.; Sand, G.; Grossmann, I. E.; Engell S. Optimization of Steel Production Scheduling with Complex Time-sensitive Electricity Cost. *Comput. Chem. Eng*. **2015**, *76*, 117.

(19) Hadera, H.; Labrik, R.; Sand, G.; Engell, S.; Harjunkoski, I. An Improved Energy-Awareness Formulation for General Precedence Continuous-Time Scheduling Models. *Ind. Eng. Chem. Res*. **2016**, *55*(5), 1336.